EMG-based multi-joint kinematics decoding for robot-aided rehabilitation therapies

Andrea Sarasola-Sanz*†, Nerea Irastorza-Landa*†, Farid Shiman*†, Eduardo López-Larraz‡, Martin Spüler§, Niels Birbaumer*¶, Ander Ramos-Murguialday*‖
*Institute of Medical Psychology and Behavioral Neurobiology, University of Tübingen, Germany
†IMPRS for Cognitive and Systems Neuroscience, Tübingen, Germany
‡I3A and Departamento de Informática e Ingeniería de Sistemas, University of Zaragoza, Spain
§Department of Computer Engineering, Wilhelm-Schickard-Institute, University of Tübingen, Germany
¶Ospedale San Camillo, Istituto di Ricovero e Cura a Carattere Scientifico, Venezia, Italy
‖TECNALIA, San Sebastian, Spain

***Abstract*—In recent years, a significant effort has been invested in the development of kinematics-decoding models from electromyographic (EMG) signals to achieve more natural control interfaces for rehabilitation therapies. However, the development of a dexterous EMG-based control interface including multiple degrees of freedom (DOFs) of the upper limb still remains a challenge. Another persistent issue in surface myoelectric control is the non-stationarity of EMG signals across sessions. In this work, the decoding of 7 distal and proximal DOFs' kinematics during coordinated upper-arm, fore-arm and hand movements was performed. The influence of the EMG non-stationarity was tested by training a continuous EMG decoder in three different scenarios. Moreover, the generalization characteristics of two algorithms (ridge regression and Kalman filter) were compared in the aforementioned scenarios. Eight healthy participants underwent EMG and kinematics recordings while performing three functional tasks. We demonstrated that ridge regression significantly outperformed the Kalman filter, indicating a superior generalization ability. Furthermore, we proved that the performance drop caused by the session-to-session non-stationarities could be significantly mitigated by including a short re-calibration phase. Although further tests should be performed, these preliminary findings constitute a step forward towards the non-invasive control of the next generation of upper limb rehabilitation robotics.**

I. Introduction

In recent years, several studies have been carried out in the field of myoelectric control for applications such as teleoperation of robots, prosthesis for amputees and rehabilitation of patients with paralyzed limbs [1], [2], [3], [4], [5], [6], [7], [8], [9], [10]. However, the development of dexterous and natural myoelectric control interfaces with multiple degrees of freedom still remains a challenge.

Most of the studies in this field have emphasized the use of EMG signals for the classification of different movement classes [1], [2]. However, these approaches have limited success when natural and smooth control of the trajectory is necessary. A decoder that maps EMG signals into a continuous profile of upper limb kinematics could overcome this limitation. Studies developing such decoders have already been performed, although most of them are limited to simple movements of either distal [3], [4], [5] or proximal [6], [7], [8] degrees of freedom (DOFs) of the upper limb. To the best of our knowledge, the only study that reported decoding of several distal and proximal DOFs of the upper limb [9] was not focused on rehabilitation approaches. Moreover, in that study target-specific and object-specific models were built for the decoding of reach-to-grasp movements, which led to high error values.

A ubiquitous issue in the field of EMG control interfaces is the non-stationarity of EMG signals that occurs across multiple sessions. Factors such as sweat, fatigue, varying upper limb configurations, electrode shift and impedance changes, could change the EMG signal distribution. This change is referred to as covariate shift and could notably affect the performance of the decoder.

In this study we aimed to decode the motion of seven DOFs (distal and proximal) of the upper limb from surface EMG signals, while participants performed different functional tasks of increasing complexity. Three different decoding schemes were implemented: within-session decoder (WS), session-to-session decoder (SS) and re-calibrated session-to-session decoder (RSS). As re-calibration was shown to improve decoding performance (e.g. by classifier adaptation [11]), a re-calibration phase using data from the beginning of the subsequent session was used to compensate for the negative effects of the session-to-session covariate shift. The performance of these three decoders was compared in order to assess the influence of the EMG non-stationarity on the decoding accuracy. Furthermore, this analysis was performed using two different algorithms, namely, ridge regression [12] and Kalman filter (KF) [13]. Up to this point, Kalman filter has been the most widely used algorithm for these applications [3], [6], [8]. However, the ridge regression technique is often underestimated and has been included in very few recent studies [4] for the decoding of EMG signals. Nevertheless, we hypothesized that, due to regularization (i.e. penalizing model complexity by imposing a constraint to the coefficients to prevent overfitting), the ridge regression technique could have a better generalization ability than the KF (i.e. predict kinematics under variable conditions more accurately).

978-1-4799-1808-9/15/$31.00

II. METHODS

A. Experimental Protocol

Eight healthy participants (3 females, 5 males, age 20-28, all right-handed) participated in this study. None of them had any neuromuscular disorder and all of them gave written consent to the procedures as approved by the ethics committee of the Faculty of Medicine of the University of Tübingen, Germany. Participants performed three different tasks while sitting and wearing a 7-DOF exoskeleton (Tecnalia, San Sebastian, Spain) on their right upper limb placed over a 70×50 cm mat. The exoskeleton allowed movements in 7 DOFs (see Fig. 1): displacement and rotation of the forearm in a 2D horizontal plane parallel to the mat's plane (3 proximal DOFs: (i) p_x position; (ii) p_y position; (iii) θ_{xy} orientation angle), pronation and supination of the wrist (1 distal DOF: (iv) ϕ_{wrist} angle) flexion and extension of the thumb, index and the group of middle, ring and pinky fingers measured as the angle of rotation with respect to the metacarpophalangeal joints (3 distal DOFs: (v) δ_{thumb}; (vi) ψ_{index}; (vii) $\alpha_{3fingers}$).

All the participants underwent two sessions that were separated by 2-9 days. During these sessions they were instructed, by means of imperative auditory cues, to perform three different tasks that always started and ended at a predefined rest position.

1) The first task consisted of reaching movements (hand relaxed) towards one of the four different targets around the mat.

2) In the second task, participants were asked to reach and point to two different targets with his/her index finger, moving towards the first target from the rest position and towards the second target immediately after reaching the first target.

3) In the third task, three objects of different shapes and sizes were located in one of the four target positions. Participants had to reach a target, grab the object placed in that position, move it to another target and then come back to the rest position. It should be noted that each of the objects required a different grasp type, which were: pinch grip, key grasp and cylindrical grasp.

Each of the tasks was divided in 5 blocks, which consisted of a set of 10-40 trials depending on the task type (40 for task 1; 10 for task 2; 22 for task 3). Resting intervals of 1-5 minutes were included between blocks in order to avoid fatigue. Participants were asked to perform the movements at their own pace and were given 4 seconds to complete task 1 trials and 6 seconds for task 2 and task 3 trials. This makes a total of approximately 30 min (task 1), 7 min (task 2) and 15 min (task 3) of recorded data per participant in each of the two sessions. It should be pointed out that, although participants performed the trials at their own pace, the aforementioned trial durations (task 1: 4 sec; task 2 and task 3: 6 sec) implied that they had to keep a rapid pace in order to accomplish the trials within the given time limits.

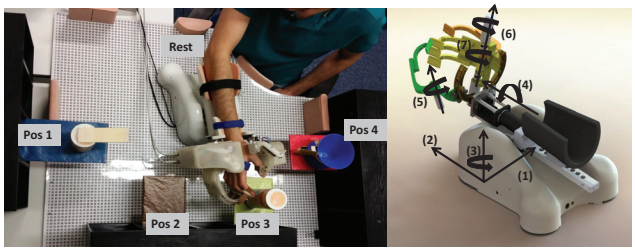

Fig. 1. (Left): Workspace where the experiments were performed. Pos1, Pos2, Pos3 and Pos4 correspond to the four targets and Rest was the predefined rest position where all the trials started and ended. (Right): Schematic of the 7 DOFs of the exoskeleton: (1) p_x; (2) p_y; (3) θ_{xy}; (4) ϕ_{wrist}; (5) δ_{thumb}; (6) ψ_{index}; (7) $\alpha_{3fingers}$

B. Data Collection

Surface EMG activity from 10 disposable bipolar electrodes (Myotronics-Noromed, Tukwila, WA, USA) over the upper-arm and fore-arm was acquired at 2500Hz using a bipolar amplifier (Brain Products GmbH, Gilching, Germany). The electrodes were placed over: 1) the abductor pollicis longus, 2) the extensor carpi ulnaris, 3) the extensor digitorium, 4) the flexor carpi radialis, palmaris longus and flexor carpi ulnaris, 5) the pronator teres, 6) the long head of biceps, 7) the external head of triceps, 8) the anterior portion of deltoid, 9) the lateral portion of deltoid and 10) the posterior portion of deltoid over the teres minor and infraespinatus muscles. The ground monopolar electrode was placed over the right clavicle. Kinematic activity of the above mentioned DOFs was recorded at 18Hz and synchronized offline with the EMG signals. The kinematics of the fore-arm DOFs, namely, p_x, p_y and θ_{xy}, were collected with a camera attached to the bottom of the exoskeleton, which tracked the movements by using an optical symbol recognition system (more details in [14]). The prono-supination angle ϕ_{wrist} was captured from a motor encoder and the fingers' angles δ_{thumb}, ψ_{index} and $\alpha_{3fingers}$ were acquired using potentiometers. Nevertheless, all the kinematic data was acquired with the same software and at the same frequency. Therefore, only the synchronization of the kinematics with the EMG signal had to be done. For this purpose, the EMG recording was initiated first. At the beginning of each block, along with the initiation of the kinematics recordings, a step signal was generated and fed into the EMG recording so that both signals could be synchronized offline.

C. Data processing

EMG data was filtered using a 4^{th} order Butterworth band-pass filter (10-500 Hz) to remove movement artifacts and high frequency noise. In addition, a 50 Hz comb filter was utilized in order to remove power line noise and its harmonics. Kinematic data was low-pass filtered with a 4^{th} order Butterworth filter (f_c = 1.5 Hz). The derivation of the positions and angles with respect to time was computed in order to obtain linear and angular velocity profiles, which were the variables to be predicted from EMG signals. The kinematic signal predicted from the decoder was filtered using a moving average with a backwards time window of

180 ms to improve movement smoothness towards online robot control.

Seven time-domain features typically used for myoelectric interfaces (Mean of absolute values, Variance, Waveform Length, Root-mean-square error, Willison Amplitude (WAMP), Zero crossing (ZC) and Slope sign changes (SSC)) [15] were extracted from each of the 10 EMG channels in 200 ms windows, resulting in a 70-element EMG feature set (7 features x 10 channels). The thresholds for the last three features were empirically selected and fixed to the same values for all the participants (TH_{WAMP} = 30 μV; TH_{ZC} = 30 μV; TH_{SSC} = 700 μV). Each of the EMG features of the generated set was normalized to zero mean and unit variance before being fed to the decoder. The testing data was normalized using the mean and standard deviation computed on the training dataset.

D. Algorithms

1) *Kalman filter*

A Kalman filter models the system by the state transition equation:

$$x_{t+1} = A_t x_t + w_t \tag{1}$$

Where x_t is the state at time t, A_t is the state transition matrix and w_t is the model white noise $\sim \mathcal{N}(0, Q)$.

The observations of the state are made through a measurement system which can be represented by the following linear equation:

$$y_t = C_t x_t + v_t \tag{2}$$

Where y_t is the observation or measurement at time t, x_t is the state at time t, C_t is the measurement matrix and v_t is additive measurement noise $\sim \mathcal{N}(0, R)$.

2) *Ridge regression*

The relationship between the dependent variable of length n, $y \in \Re^{1\times n}$, in this case velocity, and the independent variable, a p-dimensional EMG feature set $X \in \Re^{pxn}$, is modeled as follows:

$$y = \beta^T X + \beta_0 \quad \text{s.t.} \quad \sum_{j=1}^{p} \beta_j^2 \leq s \tag{3}$$

With $\beta^T \in \Re^{px1}$ being the vector of coefficients and β_0 the intercept term. The regularization consists of constraining the sum of squared coefficients with some value $s > 0$.

The solution is the one that minimizes the penalized residual sum of squares, which is expressed as:

$$\sum_{i=1}^{n}(y_i - \sum_{j=1}^{p} x_{ij}\beta_j)^2 + \lambda \sum_{j=1}^{p} \beta_j^2 \tag{4}$$

With λ being the regularization parameter. Since the penalized residual sum of squares in equation 4 is convex, it has a unique solution given by:

$$\beta_{ridge} = (X^T X + \lambda I_p)^{-1} X^T y \tag{5}$$

E. Decoding schemes

Three decoding schemes were implemented by using different training and testing conditions:

- *Within-session decoder* (WS): This decoder was trained and tested with data from the same session. It was implemented in order to have a metric of how good our decoder could work. Since we collected data during two sessions, we developed two types of decoders: one using only data from the first session S1 (WS1) and the other one only with data from the second session S2 (WS2).
- *Session-to-session decoder* (SS): This decoder was trained and validated in the first session S1 and tested in the next session S2. A performance drop due to the session-to-session transfer was expected when comparing its performance to the one of the WS decoder.
- *Re-calibrated session-to-session decoder* (RSS): This decoder was similar to the SS decoder explained above with the difference that a few minutes of data were collected at the beginning of S2 in order to re-calibrate the decoder. This was useful in order to check if this re-calibration phase could compensate for the expected performance drop due to the session-to-session transfer.

F. Cross-validation

All three of the decoding schemes were implemented for each task and DOF separately. The data from each session, task and DOF was divided into 5 blocks, each of them containing trials of all the trajectory types. These five blocks were divided into the training and test sets as follows:

For the WS decoding scheme, a 5-fold cross-validation (CV) was applied using only data from either S1 (for WS1) or S2 (for WS2). The values obtained from the testing phase of each CV-fold were averaged to compute the reported final performance. The SS decoding scheme, instead, consisted of a training phase with all 5 blocks of S1 and a testing phase with all 5 blocks of S2. For the RSS decoding scheme, all 5 blocks of S1 and the first block of S2 were included in the training set in order to re-calibrate the decoder. The remaining 4 blocks of S2 were assigned to the test set.

It should be mentioned that in the case of ridge regression, a nested CV was applied in all the decoding schemes because an optimum value for the regularization parameter had to be found. In each fold of the inner CV-loop, one of the blocks from the training set was employed as validation data in order to find the optimum regularization parameter. A grid search of values in the range $[10^{-7} - 10^{7}]$ was utilized to find the best parameter. After this, the decoder was once

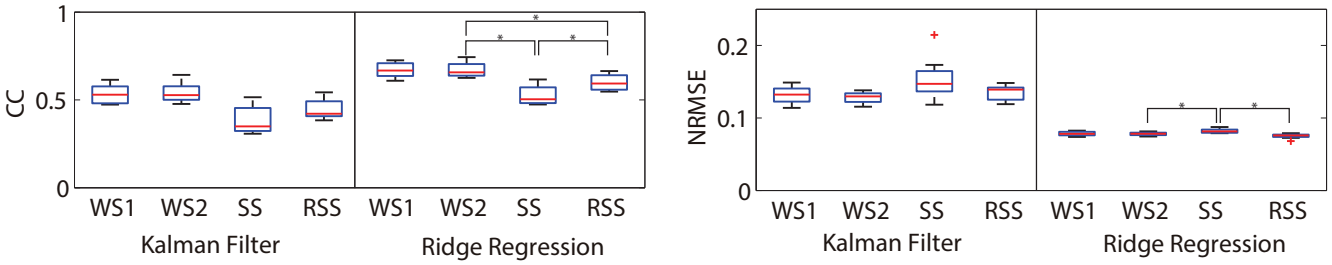

Fig. 2. Correlation coefficient (left) and normalized root mean squared error (right) for each combination of decoding scheme (WS1, WS2, SS or RSS) and algorithm (Kalman filter or ridge regression) after averaging over all subjects, tasks and involved DOFs. The median and the 25^{th} and 75^{th} percentiles are shown. Significant differences found between the decoding schemes using ridge regression are marked with an asterisk.

again trained with this optimized parameter and tested in the outer loop.

G. Performance evaluation

The correlation coefficient (CC) and the normalized root mean squared error (NRMSE) were employed as performance metrics. The reported performance values for each combination of decoding scheme and algorithm were computed as the average over the three tasks and the 8 participants. Each task's performance was in turn computed as the mean performance of the DOFs involved (i.e. actively used) in the corresponding task only.

Both for the CC and NRMSE values the following tests were applied:

Data was assumed to be normally distributed and a 2-way repeated measures Analysis of Variance (ANOVA) test with two factors (Algorithm and Decoding Scheme) was performed. The algorithm factor was comprised of two levels: Kalman filter and ridge regression while the decoding scheme factor consisted of three levels: WS2, SS and RSS.

This first test was used in order to find out which algorithm performed better overall and if that difference in performance was significant. Subsequent tests were then limited to the best algorithm. Secondly, a one-way repeated measures ANOVA was performed to test the effect of the decoding scheme factor only for the best algorithm. Post-hoc pairwise comparisons of the three decoding schemes were performed and controlled for multiple comparisons using Bonferroni correction.

For the best algorithm, a paired t-test comparing WS1 and WS2 decoding performance was also carried out in order to analyze the performance stability of the WS decoder and by extension, the reliability of session S1 and S2 data.

III. Results

For both metrics, the ANOVA resulted in a significant effect for both the algorithm (CC: $p = 10^{-6}$; NRMSE: $p = 10^{-5}$) and decoding scheme (CC: $p = 10^{-6}$; NRMSE: $p = 0.011$) factors while the interaction turned out to be non-significant (CC: $p = 0.075$; NRMSE: $p = 0.070$). The ridge regression algorithm performed significantly better than the Kalman filter and thereby, the subsequent tests were reduced to the comparison of the different decoding schemes using only ridge regression.

With the factor algorithm fixed at ridge regression, the one-way ANOVA test resulted in a significant decoding scheme effect in both cases (CC: $p < 10^{-6}$; NRMSE: $p = 10^{-5}$). Post-hoc Bonferroni corrected test results differed for each metric (see Fig. 2). For the CC, post-hoc tests revealed significant differences between the three decoding schemes. (WS2 vs SS: $p < 10^{-6}$; SS vs RSS: $p = 2.1 \cdot 10^{-4}$; WS2 vs RSS: $p = 3.1 \cdot 10^{-5}$). However, for the NRMSE metric, significant differences were found for the comparisons WS2 vs SS ($p = 4.5 \cdot 10^{-3}$) and SS vs RSS ($p = 7.5 \cdot 10^{-4}$) while the comparison WS2 vs RSS showed no significant difference ($p = 0.129$).

The paired t-test comparing WS1 and WS2 decoding schemes performance showed no significant difference for both CC ($p = 0.918$) and NRMSE ($p = 0.859$).

Additionally, for each of the three decoding schemes based on the ridge regression algorithm, the performance values (CC and NRMSE) for each of the DOFs separately were computed (see Fig. 3 and values in Table I). The performance values obtained for each DOF were consistent across decoding schemes. A significantly ($p = 10^{-6}$) lower CC for the distal DOFs (mean CC = 0.39) compared to the proximal DOFs (mean CC = 0.68) can be seen. However, the NRMSE stayed stable at a mean value of 0.077 (7.7%) for all the DOFs.

IV. Discussion

In this study, multiple decoding schemes and algorithms for the continuous mapping of EMG signals into upper limb kinematics were tested. The analysis included the decoding of distal and proximal DOFs during complex functional movements involving coordinated upper-arm and fore-arm muscle activity. Kalman filter and ridge regression techniques were compared across different decoding scenarios in order to test their ability to overcome the EMG non-stationarity as well as the variability in the performed movements. All these aspects are of great importance and have a direct impact on the clinical applications of EMG decoding.

The Kalman filter model has been extensively used before for myoelectric control applications. However, simple

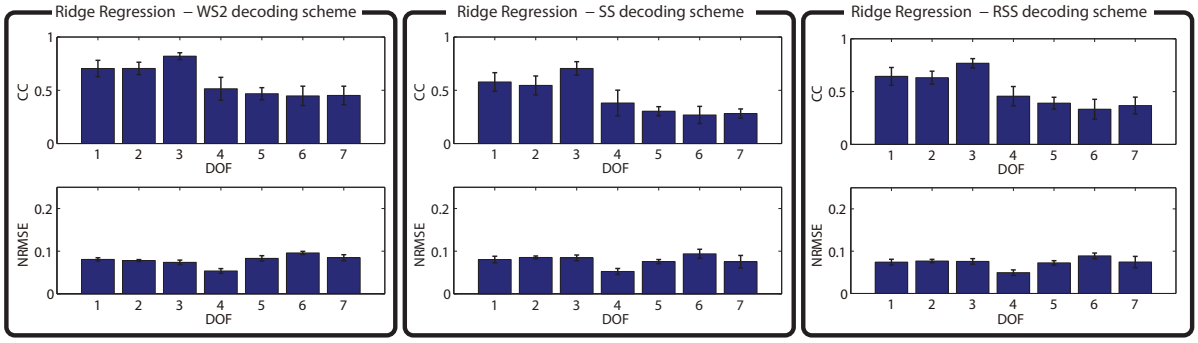

Fig. 3. Mean and standard deviation values of correlation coefficient (top) and normalized root mean squared error (bottom) for the decoded linear or angular velocities in each individual DOF, obtained with the WS2 (left), SS (middle) and RSS (right) decoding schemes. DOFs 1-2 correspond to linear velocities of: (1) p_x, (2) p_y; and DOFs 3-7 correspond to angular velocities of: (3) θ_{xy}; (4) ϕ_{wrist}; (5) δ_{thumb}; (6) ψ_{index}; (7) $\alpha_{3fingers}$.

TABLE I. MEAN AND STD VALUES OF CC AND NRMSE FOR EACH DOF AND DECODING SCHEMES USING ONLY RIDGE REGRESSION

	CC			**NRMSE**		
DOF	WS2	SS	RSS	WS2	SS	RSS
1	0.70 ($\pm$ 0.08)	0.58 ($\pm$ 0.09)	0.64 ($\pm$ 0.08)	0.081 ($\pm$ 0.004)	0.080 ($\pm$ 0.008)	0.074 ($\pm$ 0.007)
2	0.70 ($\pm$ 0.06)	0.55 ($\pm$ 0.09)	0.63 ($\pm$ 0.06)	0.078 ($\pm$ 0.002)	0.085 ($\pm$ 0.003)	0.077 ($\pm$ 0.004)
3	0.82 ($\pm$ 0.03)	0.70 ($\pm$ 0.06)	0.77 ($\pm$ 0.04)	0.074 ($\pm$ 0.005)	0.084 ($\pm$ 0.007)	0.076 ($\pm$ 0.007)
4	0.51 ($\pm$ 0.11)	0.38 ($\pm$ 0.12)	0.46 ($\pm$ 0.09)	0.054 ($\pm$ 0.006)	0.053 ($\pm$ 0.007)	0.049 ($\pm$ 0.007)
5	0.47 ($\pm$ 0.06)	0.30 ($\pm$ 0.04)	0.39 ($\pm$ 0.06)	0.083 ($\pm$ 0.006)	0.076 ($\pm$ 0.005)	0.072 ($\pm$ 0.005)
6	0.45 ($\pm$ 0.09)	0.27 ($\pm$ 0.08)	0.33 ($\pm$ 0.09)	0.096 ($\pm$ 0.004)	0.094 ($\pm$ 0.011)	0.089 ($\pm$ 0.007)
7	0.45 ($\pm$ 0.08)	0.28 ($\pm$ 0.04)	0.37 ($\pm$ 0.08)	0.085 ($\pm$ 0.007)	0.075 ($\pm$ 0.015)	0.074 ($\pm$ 0.013)

algorithms like ridge regression are often underestimated and therefore excluded from EMG decoding studies. Regularization methods impose a constraint to the model coefficients (i.e. control how large the coefficients are). This introduces the advantage of preventing overfitting and thus, of having a model with good generalization characteristics. This is highly desirable, especially in situations in which the decoder should be able to generalize to movements from which sufficient training data is not available. The results of the work presented here confirm our hypothesis that ridge regression generalizes to new EMG data better than the Kalman filter. Therefore, ridge regression constitutes a desirable algorithm for the continuous EMG decoding of upper limb kinematics.

Factors such as external interference, electrode shift and lift, electrode impedance changes, muscle fatigue, sweat and varying upper-limb positions alter the EMG signal distribution. Sources of variation like external interference can be mostly suppressed by filtering or electromagnetic shielding techniques. However, the remaining sources constitute a persistent issue in clinical practice and severely affect the performance of myoelectric decoders. In fact, we believe that in this particular study, one of the main factors affecting the performance stability could have been the variable positioning of the EMG electrodes from session-to-session since they were just placed within the general vicinity. A daily re-calibration phase was proposed as a solution to alleviate the effects of such non-stationarities. The additional time of re-calibrating the decoder and the cost of recording new data at the beginning of each session could be a concern for certain applications. Nevertheless, the performance comparisons between the three developed decoding schemes showed that there was a significant improvement in performance (a 14% increase in CC and a 8% reduction in NRMSE with respect to SS) when a re-calibration of the decoder was carried out. Moreover, the NRMSE values of the re-calibrated decoder were not significantly different from those achieved when training and testing the decoder with data from the same session (WS2 decoder). This implies that a re-calibration phase could reduce the error to the extent that the values would be just as low as if the decoder was trained using a larger amount of data only from the current session. It should also be mentioned that the calibration data length was 5 min, 1.5 min and 3 min for each task respectively and that it took a negligible amount of time to build the decoding model and choose the optimal regularization parameter, as opposed to other more complex algorithms. Therefore, the proposed approach was not very time and computationally demanding and served to significantly raise the performance. Nonetheless, the benefits and disadvantages of including a daily re-calibration phase should be carefully considered in order to choose the most suitable approach for each particular scenario.

The majority of recent studies in the field of myoelectric control interfaces are constrained to the decoding of a few distal or proximal DOFs. These devices could be employed for those cases in which impaired function of a few specific DOFs is present. However, the ability for interfaces to control multiple DOFs of the upper limb during dexterous and functional movements is necessary, especially for patients who are undergoing rehabilitation therapies for motor impairment of an entire extremity. Our protocol included the

decoding of coordinated multi-joint movements. While the NRMSE was stable at a very low value for all the DOFs, the lower CC values achieved for the distal DOFs might be due to the limited number of electrodes used for the decoding of distal DOFs. Extensors and flexor muscles of the forearm are often more difficult to target and it is usually hard to isolate the EMG activity from each recorded muscle. This makes the discrimination and decoding of individual finger movements more challenging. The minimum number of electrodes on the forearm that are necessary to attain an accurate decoding of distal DOF movements has been extensively investigated before [1], [4], [16], [17]. From the results presented in these previous studies, it can be concluded that a minimum of 12-16 electrodes are necessary to distinguish between multiple individual finger and wrist movements. Therefore, future studies should be performed with additional electrodes placed over the fore-arm in order to improve the decoding accuracy of distal DOFs.

V. Conclusion

This study addressed important aspects for the use of myoelectric control interfaces in clinical practice, which were: (i) the choice of a decoding algorithm with good generalization characteristics; (ii) the training procedure to follow in order to develop a decoder, which is robust to non-stationarities; and (iii) the decoding of coordinated distal and proximal DOF movements during complex functional tasks. From the results presented here, we concluded that a simple regularized algorithm such as ridge regression has good generalization characteristics for the EMG-based continuous decoding of multiple DOFs of the upper limb. Moreover, we demonstrated that by introducing a daily re-calibration phase the effects of the session-to-session non-stationarities could be significantly mitigated. Further studies including additional electrodes over the fore-arm should be performed in order to more accurately discriminate individual finger movements. Nevertheless, this pilot study is an important step towards the development of a robust myoelectric interface for the online control of coordinated multi-joint movements in robot-aided rehabilitation therapies.

Acknowledgment

This study was funded by the Baden-Württemberg Stiftung (GRUENS), the Indian-European collaborative research and technological development projects (INDIGO-DTB2-051), the Natural Science Fundation of China (NSFC 31450110072), EU COST action TD1006, Deutsche Forschungsgemeinschaft (DFG, Koselleck), Eva und Horst Köhler Stiftung, Volkswagen Stiftung and Bundes Ministerium für Bildung und Forschung BMBF MOTOR-BIC (FKZ 13GW0053). A. Sarasola-Sanz's work is supported by La Caixa-DAAD scholarship, E. López-Larraz's work by the Spanish projects HYPER-CSD2009-00067 and DGA-FSE (grupo T04) and N. Irastorza-Landa's work by the Basque Government and IKERBASQUE, Basque Foundation for Science, Bilbao, Spain.

References

[1] F. Tenore, A. Ramos, S. Fahmy, A.and Acharya, R. Etienne-Cummings, and N. Thakor, "Decoding of individuated finger movements using surface electromyography," *IEEE Transactions on Biomedical Engineering*, vol. 56, no. 5, pp. 1427 – 1434, 2009.

[2] S. W. Lee, K. Wilson, and D. Lock, B.A.and Kamper, "Subject-specific myoelectric pattern classification of functional hand movements for stroke survivors," *IEEE Transactions on Neural Systems and Rehabilitation Engineering*, vol. 19, no. 5, pp. 558 – 566, 2010.

[3] E. A. Corbett, E. J. Perreault, and K. P. Krding, "Mixture of time-warped trajectory models for movement decoding," *Advances in Neural Information Processing Systems 23 (NIPS)*, 2010.

[4] J. Hahne, F. BieBmann, N. Jiang, H. Rehbaum, D. Farina, F. Meinecke *et al.*, "Linear and nonlinear regression techniques for simultaneous and proportional myoelectric control," *IEEE Transactions on Neural Systems and Rehabilitation Engineering*, vol. 22, no. 2, pp. 269–279, 2014.

[5] R. Smith, F. Tenore, D. Huberdeau, R. Etienne-Cummings, and N. Thakor, "Continuous decoding of finger position from surface EMG signals for the control of powered prostheses." in *30th Annual International Conference of the IEEE Engineering in Medicine and Biology Society, EMBS*, 2008, pp. 197 – 200.

[6] P. Artemiadis and K. Kyriakopoulos, "A bio-inspired filtering framework for the EMG-based control of robots," *17th Mediterranean Conference on Control and Automation*, pp. 1155–1160, 2009.

[7] P. K. Artemiadis and K. J. Kyriakopoulos, "A switching regime model for the EMG-based control of a robot arm," *IEEE Transactions on Systems, Man, and Cybernetics*, vol. 41, no. 1, pp. 53–63, 2010.

[8] N. Sachs, E. Corbett, L. Miller, and E. Perreault, "Continuous movement decoding using a target- dependent model with EMG inputs," *Annual International Conference of the IEEE EMBC*, pp. 5432–5435, 2011.

[9] M. V. Liarokapis, P. K. Artemiadis, K. J. Kyriakopoulos, and E. S. Manolakos, "A learning scheme for reach to grasp movements: On EMG-based interfaces using task specific motion decoding models," *Biomedical and Health Informatics*, vol. 17, no. 5, pp. 915–921, 2013.

[10] A. Ramos-Murguialday, E. Garca-Cossio, A. Walter, W. Cho, D. Broetz, M. Bogdan, L. G. Cohen, and N. Birbaumer, "Decoding upper limb residual muscle activity in severe chronic stroke," *Annals of Clinical and Translational Neurology*, vol. 2, no. 1, pp. 1 – 11, 2015.

[11] M. Spüler, W. Rosenstiel, and M. Bogdan, "Adaptive SVM-based classification increases performance of a MEG-based brain-computer interface (BCI)," in *Artificial Neural Networks and Machine Learning–ICANN 2012*. Springer, 2012, pp. 669–676.

[12] A. E. Hoerl and R. W. Kennard, "Ridge regression: Biased estimation for nonorthogonal problems," *Technometrics*, vol. 12, no. 1, pp. 55–67, 1970.

[13] R. Kalman, "A new approach to linear filtering and prediction problems," *Journal of basic Engineering*, vol. 82, pp. 35 – 45, 1960.

[14] H. Zabaleta, D. Valencia, J. Perry, J. Veneman, and T. Keller, "Absolute position calculation for a desktop mobile rehabilitation robot based on three optical mouse sensors," *Annual International Conference of the IEEE Engineering in Medicine and Biology Society, EMBC*, pp. 2069 – 2072, 2011.

[15] M. Zecca, S. Micera, M. C. Carrozza, and P. Dario, "Control of multifunctional prosthetic hands by processing the electromyographic signal," *Critical Review in Biomedical Engineering*, vol. 30, pp. 4 – 6, 2002.

[16] S. Maier and P. van der Smagt, "Surface EMG suffices to classify the motion of each finger independently," *Proceedings of the International Conference of Motion and Vibration Control, MOVIC*, 2008.

[17] H. Daley, K. Englehart, L. Hargrove, and U. Kuruganti, "High density electromyography data of normally limbed and transradial amputee subjects for multifunction prosthetic control," *Journal of Electromyography and Kinesiology*, vol. 22, no. 3, pp. 478 – 484, 2012.